



Transactions of the 13th International Conference on Structural Mechanics in Reactor Technology (SMiRT 13), Escola de Engenharia - Universidade Federal do Rio Grande do Sul, Porto Alegre, Brazil, August 13-18, 1995

Fracture evaluation of a crack in the service water piping system to an emergency diesel generator

Rudland, D., Scott, P., Rahman, S., Wilkowski, G.
Batelle Memorial Institute, Columbus, Ohio, U.S.A.

ABSTRACT: A pipe fracture experiment was conducted on a section of 6-inch nominal diameter pipe which was degraded by microbiologically induced corrosion (MIC) at a circumferential girth weld. The pipe was a section of one of the service water piping systems to one of the emergency diesel generators at the Haddam Neck (Connecticut Yankee) plant. The experimental results will help validate future ASME Section XI pipe flaw evaluation criteria for other than Class 1 piping. A critical aspect of this experiment was an assessment of the degree of conservatism embodied in the ASME definition of flaw size. The ASME flaw size definition assumes a rectangular shaped, constant depth flaw with a depth equal to its maximum depth for its entire length. Since most service flaws are very irregular in shape, this definition can be very conservative. Alternative equivalent flaw size definitions for irregular shaped flaws are explored in this paper.

INTRODUCTION

The accuracy of pipe fracture analyses is highly dependent on the size and shape of the defect. How a fracture analyst estimates the length and depth of a "real-world" surface flaw can be as important as the estimate of the loads on the pipe for an inservice flaw assessment. The pipe fracture data developed in the past have been developed using well-controlled test conditions. The flaws generally have been machined flaws, which were relatively uniform in depth. Some were fatigue precracked to provide a sharp crack. The pipe wall thicknesses also tended to be fairly uniform. However, in reality, flaws that occur in service tend to have irregular depths. It is up to the analyst to make a valid approximation of the flaw size for use in an appropriate fracture analysis procedure. The objective of this effort was to conduct a pipe experiment on a section of 6-inch nominal diameter pipe donated by Northeast Utilities. The pipe was removed from the service water system of the Haddam Neck (Connecticut Yankee) Plant due to degradation caused by microbiologically induced corrosion (MIC) and a crack at a girth weld.

The rationale for conducting this pipe experiment was to allow for an assessment of the significance of an actual girth-weld defect, possibly enhanced by microbiologically induced corrosion, on the integrity of piping. The data from this experiment provided a "real-world" assessment of the analysis methodologies developed to date for the assessment of degraded piping. In this pipe, both the wall thickness and crack depth were highly non-uniform. The depth of the flaw ranged from 7.0 to 63.5 percent of the wall thickness, based on ultrasonic inspections carried out by inspectors at Northeast Utilities. Both of these factors, i.e., the non-uniform wall thickness and the irregular flaw size, complicated the analysis of

this experiment. However, these are the types of complicating factors that a plant engineer must often face. Consequently, data from this experiment provide insight into the uncertainties in the pipe fracture analyses that may occur due to practical considerations.

PIPE FRACTURE EXPERIMENT

The pipe section from the Haddam Neck Plant service water piping system was a 6-inch nominal diameter, Schedule 40, A53 Grade A carbon steel pipe that was 240-mm (9.5-inches) long. It was shielded-metal arc welded on one end to a 150-pound class weld neck flange. The flaw was in the pipe-to-flange girth weld. In addition, a long-radius elbow was welded to the other end of the pipe section. Figure 1 is a schematic showing this section of pipe.

Prior to the experiment, both welds were ultrasonically and radiographically inspected to determine the pipe wall thickness and crack depth using a nuclear-certified inspectors from Northeast Utilities. Once the inspections were completed, moment arms were welded onto the test specimen in preparation for testing.

Tensile, Charpy and fracture toughness specimens were machined from the base metal, while fracture toughness and Charpy specimens were machined from the elbow-pipe girth weld to characterize the materials. Table 1 shows a summary of these results. Details of these results can be found in Reference 1.

RESULTS FROM THE PIPE EXPERIMENT

The cracked-pipe specimen was loaded in four-point bending. The test specimen was aligned in the load frame such that the deepest part of the crack would be in the region of maximum bending stress from the applied bending loads. In addition to the bending loads, the internal pipe pressure was maintained at a constant value of 0.7 MPa (100 psi), the operation pressure of the service water piping system. The test temperature was ambient, i.e., 16 C (60 F).

The maximum moment for this experiment was 60.37 kN-m. Table 2 presents the key results for this experiment. Included in Table 2 are the pipe and crack dimensions, the moment at crack initiation, and the maximum moment for the experiment.

RESULTS OF THE ANALYSIS EFFORTS FOR THE PIPE EXPERIMENT

The maximum moment from this pipe experiment was compared with predictions of maximum moment using the following analysis methods:

SC.TNP1 and SC.TNP2^(2,3)

SC.ENG1 and SC.ENG2⁽³⁾

R6 Revision 3 Option 1⁽⁴⁾

Net-Section-Collapse (NSC)⁽⁵⁾

Dimensionless-Plastic-Zone-Parameter (DPZP)⁽⁶⁾

ASME Section XI Appendix H and IWB-3650⁽⁷⁾.

Details of each of these analysis methods can be found in the appropriate references.

In making predictions for this experiment, quasi-static base metal tensile data and quasi-static weld metal J-R curve data were used. For these predictions the flow stress was defined as the average of the yield and ultimate strengths. For the J-estimation schemes, i.e., SC.TNP and SC.ENG, and R6 predictions, the base metal stress-

strain curve behavior was modeled using a Ramberg-Osgood relationship where the Ramberg-Osgood equation was fit to the stress-strain data in the range from 0.1-percent strain to the strain corresponding to 80 percent of the ultimate strength.

Prior to the conduct of the pipe experiment, the test specimen was inspected by personnel at Northeast Utilities. They measured the wall thickness of the pipe near the pipe-to-flange girth weld, to quantify the extent of the microbiologically induced corrosion, and measured the depth of the crack in this weld at approximately 20 locations around the pipe circumference using ultrasonic testing (UT) techniques. After the pipe test, the girth weld flaw was measured optically at the same locations. These measurements are shown in Figure 2.

As can be seen in Figure 2, the crack in the weld extended all the way around the pipe circumference and was approximately 63.5 percent of the pipe wall thickness in depth at its deepest location. The wall thickness of this nominal 7.11-mm (0.280-inch)-thick pipe had been reduced by the MIC and general corrosion such that the actual wall thickness ranged from 5.08 mm (0.200 inch) at its thinnest location to 6.48 mm (0.255 inch) at its thickest location. A number of different crack size and wall thickness definitions were used in making these predictions, see Table 3. Unless otherwise noted, the predictions were based on the optical measurements made after the specimen had been broken open. As can be seen in Figure 2, the ultrasonically determined crack depths measured before the experiment were not that different from those measured optically after the experiment.

The wall thickness measurements shown in Table 3 for Cases 1 through 4 are the actual measured wall thicknesses at the deepest location, without the weld crown, measured posttest using a set of micrometers. The wall thickness measurements for Cases 5 through 8 are similar to those for Cases 1 through 4, respectively, except the wall thickness measurements for Cases 5 through 8 include the height of the weld crown. For each case the crack depth is the depth of the crack at its deepest location. For Cases 1 and 5, the crack length is the total length of the crack, i.e., 360 degrees in both cases. For Cases 2 and 6, the length of the crack is established on an equivalent crack length basis, where the equivalent crack length is defined as the total cracked area divided by the maximum crack depth. For Cases 3 and 7, the length of the crack is also established on an equivalent crack length basis where the equivalent crack length is defined as the area of the crack above the neutral bending axis of the crack section divided by the maximum crack depth. For Cases 4 and 8, the length of the crack is set at 50 percent of the pipe circumference, which is the same as a 100-percent circumferential length crack in Article IWB-3650 of Section XI of the ASME Code. The final case shown in Table 3 (Case 9) is similar to Case 3 (i.e., maximum crack depth, equivalent crack length using only the area above the neutral bending axis, and wall thickness without weld crown height) except the crack dimensions are based on pretest ultrasonic inspection results instead of the posttest optically measured crack size.

The predictions of the maximum moments using the J-estimation scheme predictions were made with the aid of a Battelle-written computer code, NRCPIPES, Version 2.0. The results of those predictions and the comparisons with the experimental results are shown in Table 4. For the ASME Appendix H procedures, a safety factor of 1.0 was used for these calculations.

In examining Table 4, it can be seen that most of the analyses for most of the pipe and flaw geometry definitions underpredicted the experimental maximum moment. The pipe and flaw geometry definition that resulted in the most accurate prediction of the maximum moment is Case 7, i.e., the pipe diameter and wall thickness measurements include the height of the weld crown, and the crack length is an equivalent crack length where the equivalent crack length is the area of the crack above the neutral axis divided by the maximum crack depth. The most inaccurate predictions are for Case 1, in which the pipe diameter and wall thickness measurements do not consider the

weld crown and the crack length is assumed to be the maximum depth for 360 degrees, i.e., all the way around the pipe circumference. As can be seen in Table 4, even for the analysis methods which in the past have been found to be the most accurate of methods considered⁽³⁾, i.e., DPZP and SC.TNP1, using the Case 1 wall thickness and crack size definitions resulted in predictions which were only about half of the actual values. It is also of note from Table 4 that the difference in fracture predictions between the case, where the crack depth was determined optically (Case 3) and ultrasonically (Case 9), is insignificant, i.e., typically less than 5 percent. This is encouraging in that it showed that in this case, the qualified inspection results provided sufficiently accurate information to make good predictions of the moment-carrying capacity of a flawed pipe even for the "real-world" case where the pipe wall and crack dimensions were highly nonuniform.

It is also of note from Table 4 that the ASME Appendix H criteria (with a safety factor of 1.0 and using Code default properties) significantly underpredict the maximum experimental moments for all cases considered. For Case 1 in Table 4, the predicted maximum moment was one-third of the experimental value.

CONCLUSIONS

A pipe bend test was conducted on a section of pipe removed from the service water system at the Haddam Neck (Connecticut Yankee) plant. The pipe section was degraded by microbiologically induced corrosion and contained a girth weld crack. The analysis of this pipe test showed that accurate predictions of maximum load-carrying capacity can be made if the maximum crack depth is known, an accurate estimate of the crack length can be made, and if the total wall thickness (including weld crown) is used in the analysis since the flaw was in the center of the weld. However, the ASME Appendix H method significantly underpredicted the maximum moment for all cases.

ACKNOWLEDGMENTS

This work was supported by the U. S. Nuclear Regulatory Commission through the Electrical, Materials and Mechanical Engineering Branch, Division of Engineering Technology, Office of Nuclear Regulatory Research. We would like to thank Mr. M. Mayfield of the NRC for his support of this work. The authors also wish to thank Northwest Utilities for donating the section of pipe used in the experiment described in this paper. Mr. Nelson Azevedo and Mr. Matthew Kupinski were especially helpful in this effort. Finally, we wish to thank Mrs. V. Kreachbaum for typing and preparing the document.

REFERENCES

1. Wilkowski, G., and others, "Short Cracks in Piping and Piping Welds," Seventh Semiannual Program Report, NUREG/CR-4599, Vol. 4, No. 1, (in press).
2. Scott, P. M., and Ahmad, J., "Experimental and Analytical Assessment of Circumferentially Surface-Cracked Pipes Under Bending," NUREG/CR-4872, BMI-2149, April 1987.
3. Krishnaswamy, P., and others, "Fracture Behavior of Short Circumferentially Surface-Cracked Pipe," NUREG/CR-6298, (in press).
4. Milne, I., and others, "Assessment of the Integrity of Structures Containing Defects," Central Electricity Generating Board, UK, R/H/R6 - Rev. 3, May 1986.

5. Kanninen, M. F., and others, "Instability Predictions for Circumferentially Cracked Type 304 Stainless Steel Pipes Under Dynamic Loadings," Final Report on EPRI Project T118-2, by Battelle Columbus Laboratories, EPRI Report Number NP-2347, April 1982.
6. Wilkowski, G. M., and Scott, P. M., "A Statistical Based Circumferentially Cracked Pipe Fracture Mechanics Analysis for Design or Code Implementation," *Nuclear Engineering and Design*, 111, pp 173-187, 1989.
7. ASME Boiler and Pressure Vessel Code, Section XI, Appendix H, American Society of Mechanical Engineers, 1992.

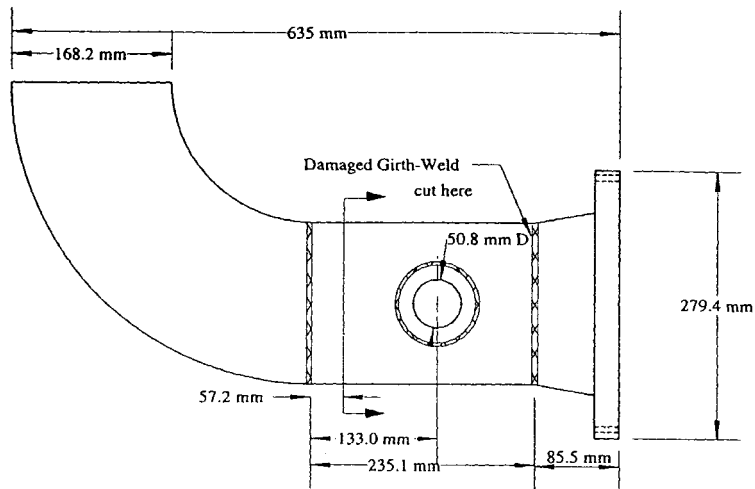


Figure 1. Schematic of pipe section removed from the Service Water Piping System of the Haddam Neck (Connecticut Yankee) Plant

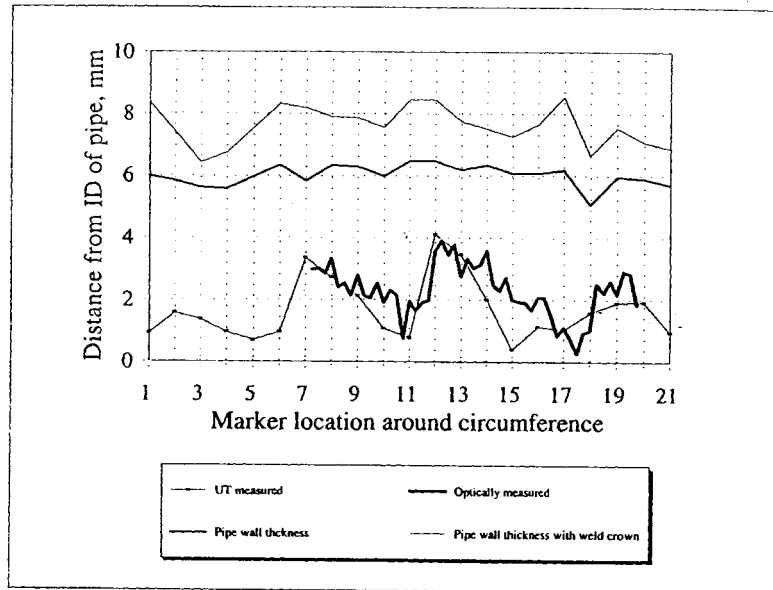


Figure 2. Wall thickness and crack depth dimensions from both ultrasonic and optical measurements

Table 1. Summary of material properties at 20 C (68 F) for the 6-inch nominal diameter service water piping system from the Haddam Neck (Connecticut Yankee) Plant

Material	0.2-Percent Offset Yield Strength,		Ultimate Tensile Strength,		J_i ,		dJ/da ,		Charpy ^(a) Upper Shelf,	
	MPa	ksi	MPa	ksi	kJ/m ²	in-lb/in ²	MJ/m ³	in-lb/in ³	J	ft-lbs
Base Metal	303.4	44.0	456.3	66.2	185.1	1,057	123.9	17,970	22	16
Weld Metal	-	-	-	-	83.6	477	110.1	15,960	15	11

(a) Charpy specimens were subsized.

Table 2. Key results for the Haddam Neck MIC pipe experiment

Pipe Diameter, mm	Wall Thickness, mm	a/t	$2c/\pi D$	Moment at Crack Initiation, kN-m (in-kip)	Maximum Moment, kN-m (in-kip)
168.7 ^(a)	6.02 ^(b)	0.60 ^(c)	1.0	59.28 (524.7)	60.37 (534.3)

(a) Excluding crown.

(b) Average value and excluding crown.

(c) Maximum crack depth divided by pipe wall thickness at the location the maximum crack depth.

Table 3. Pipe and crack size definitions used in the fracture prediction analyses

Case Number	Wall Thickness Includes Weld Crown	Wall Thickness, mm	Crack Size Measured Optically or Ultrasonically	Crack Depth	a_{max}/t	Crack Length	$2c/\pi D$
	Yes/No						
1	No	6.48	Optically	a_{max}	0.605	360°	1.0
2	No	6.48	"	"	0.605	Equivalent ^(a)	0.49
3	No	6.48	"	"	0.605	Equivalent ^(b)	0.359
4	No	6.48	"	"	0.605	180°	0.50
5	Yes	8.12	"	"	0.483	360°	1.0
6	Yes	8.12	"	"	0.483	Equivalent ^(a)	0.49
7	Yes	8.12	"	"	0.483	Equivalent ^(b)	0.346
8	Yes	8.12	"	"	0.483	180°	0.50
9	No	6.48	Ultrasonically	"	0.635	Equivalent ^(b)	0.288

(a) Total crack area/maximum crack depth.

(b) Crack area above neutral axis/maximum crack depth.

Table 4. Predicted maximum moments from analyses of the MIC pipe test^(a)

Method	Maximum Moment, kN-m								
	Case 1	Case 2	Case 3	Case 4	Case 5	Case 6	Case 7	Case 8	Case 9
NSC	34.72	38.14	43.35	37.84	55.09	57.28	62.53	57.03	46.02
DPZP	33.56	36.86	41.90	36.57	53.20	55.32	60.40	55.07	44.50
SC.TNP1	38.16	38.63	42.77	38.39	56.87	55.79	60.03	55.65	44.96
SC.TNP2	29.37	29.79	32.97	29.60	44.90	43.95	47.05	43.86	34.60
SC.ENG1	28.45	32.47	37.55	32.17	46.67	50.48	56.22	50.20	39.75
SC.ENG2	25.77	27.88	30.26	27.75	43.23	45.79	49.11	45.64	30.15
R6 Rev. 3 Opt.1	31.58	33.15	37.35	32.91	50.23	50.00	54.55	49.77	39.21
ASME ^(b)	20.13	20.30	23.15	20.13	30.74	30.22	33.79	30.74	24.62

(a) Maximum experimental moment = 60.37 kN-m (534.3 in-kips).

(b) Appendix H analysis using Material Category 1 default properties and a safety factor of 1.0.